

Multimodal imaging with ^{18}F -FDG-PET/CT and ^{111}In -Octreotide SPECT in patients with metastatic medullary thyroid carcinoma

Serena De Luca¹ · Rosa Fonti² · Luigi Camera¹ · Barbara Salvatore² ·
Antongiulio Faggiano³ · Andrea Ciarmiello⁴ · Sabrina Segreto¹ · Annamaria Colao³ ·
Marco Salvatore⁵ · Silvana Del Vecchio^{1,2}

Received: 15 September 2015 / Accepted: 13 December 2015 / Published online: 11 January 2016
© The Japanese Society of Nuclear Medicine 2016

Abstract

Objective The aim of our study was to determine the role of fluorine-18 fluorodeoxyglucose positron emission tomography/computed tomography (^{18}F -FDG-PET/CT) and indium-111 Octreotide single photon emission tomography (^{111}In -Octreotide SPECT) in the evaluation of metastatic medullary thyroid carcinoma (MMTC).

Methods Twenty-five MMTC patients were retrospectively evaluated. All patients had undergone whole-body ^{18}F -FDG-PET/CT including 20 who had also undergone ^{111}In -Octreotide SPECT within a maximum interval of 6 weeks. Diagnostic contrast-enhanced computed tomography (CT) alone or as part of ^{18}F -FDG-PET/CT examination was performed in all patients.

Results Contrast-enhanced CT detected a total of 131 lesions including 79 enlarged lymph nodes and 14 bone lesions. ^{18}F -FDG-PET/CT visualized a total of 92 true positive lesions (SUV_{max} range 1.1–10.0, mean 4.0 ± 1.7) including 66 lymph nodes, 7 of which were not enlarged on CT, and 8 bone metastases. In the 20 patients studied with both techniques, a total of 64 and 46 true positive lesions

were detected by ^{18}F -FDG-PET/CT and ^{111}In -Octreotide SPECT, respectively. In particular, ^{18}F -FDG uptake was found in 43 lymph nodes and in 7 bone metastases whereas ^{111}In -Octreotide uptake was detected in 27 lymph nodes and in 10 bone metastases.

Conclusions In MMTC patients, ^{18}F -FDG-PET/CT provides a useful contribution mainly in evaluating lymph node involvement whereas ^{111}In -Octreotide SPECT can contribute to the detection and somatostatin receptor characterization especially of bone lesions.

Keywords Medullary thyroid carcinoma · ^{18}F -FDG-PET/CT · ^{111}In -Octreotide SPECT · Contrast-enhanced CT · Multimodal imaging

Introduction

Medullary thyroid carcinoma (MTC) is a rare cancer arising from neural crest derived parafollicular C cells of the thyroid gland. It accounts for less than 5 % of all thyroid cancers and occurs in both a sporadic (80 %) and a familial form (20 %) [1, 2]. MTCs may have a variable biological behavior from indolent slow-growing tumors to highly aggressive types [2]. Almost all MTCs synthesize and secrete the polypeptide hormone calcitonin that serves as a biomarker of tumor burden. Detectable or increasing levels of calcitonin during the follow-up of MTC patients who had undergone curative total thyroidectomy and extensive lymph node dissection, indicate persistent, recurrent or metastatic disease [3, 4].

Distant metastases are the main cause of death in MTC patients. Survival after the discovery of distant metastases is around 25 % at 5 years and 10 % at 10 years [5]. Distant metastases are observed at presentation in 7–23 % of

✉ Silvana Del Vecchio
delvecc@unina.it

¹ Department of Advanced Biomedical Sciences, University of Naples Federico II, Via Pansini 5, Edificio 10, 80131 Naples, Italy

² Institute of Biostructures and Bioimages, National Research Council, Naples, Italy

³ Department of Clinical Medicine and Surgery, University of Naples Federico II, Naples, Italy

⁴ Nuclear Medicine Department, Hospital S. Andrea, La Spezia, Italy

⁵ IRCCS-SDN, Naples, Italy

patients or after initial treatment in one to two-thirds of patients with persistently elevated calcitonin levels at different time intervals depending on progression rate of the disease [5, 6]. They are often multiple in the involved organs and simultaneously affect multiple organs including lungs, liver and bones.

Accurate localization of distant metastases is of primary importance for the management of patients with metastatic MTC and several imaging modalities are employed to assess the full extent of disease and to guide therapeutic intervention [7, 8]. On the basis of imaging findings patients are considered candidates for systemic treatment preceded or not by additional local interventions, and tumor response of all relevant sites of disease can be monitored by imaging. The work-up of patients with metastatic MTC may include neck ultrasound, neck and chest CT, liver triphase contrast-enhanced CT or contrast-enhanced magnetic resonance imaging (MRI), bone scintigraphy and MRI of spine and pelvis [5, 6]. Recently functional imaging with ^{18}F -FDG-PET and PET/CT has been used for the detection of recurrent or metastatic sites of MTC [9]. According to a meta-analysis of 15 studies, the pooled sensitivities of ^{18}F -FDG-PET and PET/CT were 68 and 69 %, respectively [10]. Detection rate of ^{18}F -FDG-PET and PET/CT was reported to increase with serum calcitonin levels ≥ 1000 pg/mL [11–13]. Despite the sub-optimal sensitivity, ^{18}F -FDG-PET or PET/CT is performed in patients with biochemical evidence of disease when cross-sectional morphological imaging fails to detect sites of disease or in patients with known metastatic MTC to evaluate disease extension [14]. Furthermore, the recent development of targeted therapy for locally advanced or metastatic MTC including tyrosine kinase inhibitors such as vandetanib [15], cabozantinib [16], sorafenib [17] and sunitinib [18] has provided an additional rationale for the use of ^{18}F -FDG-PET or PET/CT in MTC patients. A high standardized uptake value (SUV_{max}) on ^{18}F -FDG-PET images may indicate a more aggressive disease requiring treatment with these drugs. Furthermore metabolic tumor response has been reported to precede the morphostructural changes after treatment with targeted agents in a number of malignancies including medullary thyroid carcinoma [19, 20].

The expression of somatostatin receptors on most MTCs [21–23] has provided the molecular basis for the use of radiolabeled somatostatin analogs such as ^{111}In -Octreotide that binds with high affinity to somatostatin subtype receptor 2 (SST2). Previous studies tested the role of imaging with ^{111}In -Octreotide in the diagnosis of residual, recurrent and metastatic foci of MTC, reporting a wide range of sensitivity between 37 and 90 % [24–28]. Many factors may account for such variability in the detection rate including lesion size and location, SST2 receptor

incidence and density and the use of planar or tomographic imaging. The aim of the present study was to evaluate the role of multimodal imaging with ^{18}F -FDG-PET/CT in the assessment of number, anatomic sites and metabolic activity of metastatic lesions and to test whether the combination with ^{111}In -Octreotide SPECT provides useful additional information in patients with MMTC.

Patients and methods

We reviewed retrospectively the medical records of 25 consecutive patients (12 women, 13 men; mean age \pm SD, 60 ± 16 years; range 24–85) with MMTC. The work-up of these patients at our institution usually includes both ^{18}F -FDG-PET/CT and ^{111}In -Octreotide SPECT in addition to CT and conventional imaging. All patients had undergone whole-body ^{18}F -FDG-PET/CT including 20 who had also undergone ^{111}In -Octreotide SPECT within a maximum interval of 6 weeks (mean \pm SD 1.9 ± 1.2 , range 1–6 weeks). Due to extensive disease, five patients were subjected to systemic treatment after ^{18}F -FDG-PET/CT scan and did not undergo combined imaging with ^{111}In -Octreotide SPECT. All patients underwent contrast-enhanced CT alone or as part of ^{18}F -FDG-PET/CT examination. Written informed consent was obtained from all patients in this study.

Initial diagnosis was obtained by histopathological examination of tumor samples obtained by total thyroidectomy in 23 patients and by core biopsy in 2 patients. None of the patients had received therapy in the 6 months before the imaging studies. Levels of calcitonin at the time of the imaging examinations were also recorded and SUV_{max} values of the most FDG-avid lesion in patients with calcitonin levels higher or lower than 1000 pg/mL were compared by using unpaired Student's *t* test. $p < 0.05$ was considered statistically significant.

^{18}F -FDG-PET/CT study

^{18}F -FDG-PET/CT scans were acquired after fasting for 8 h and 60 min after i.v. injection of ^{18}F -FDG (370 MBq). The blood glucose level, measured just before tracer administration, was < 120 mg/dL in all patients. ^{18}F -FDG-PET/CT images were obtained using a combined PET/CT Discovery LS scanner (GE Healthcare, Milan, Italy) as previously described [29].

All areas of focal ^{18}F -FDG uptake visible on 2 contiguous PET slices at least and not corresponding to physiological tracer uptake were considered to be positive [30]. Maximum standardized uptake values (SUV_{max}) of all focal lesions were recorded.

¹¹¹In-Octreotide SPECT

¹¹¹In-Octreotide was prepared using the commercially available kit OctreoScan (Covidien Italia S.p.A., Segrate, Milan, Italy) following the manufacturer's instructions. Images were obtained at 4 and 24 h after injection of ¹¹¹In-Octreotide (200 MBq) using a dual-head large-FOV gamma camera (ECAM, Siemens) equipped with medium-energy parallel-hole collimators and 20 % energy windows centered on ¹¹¹In-photopeaks (172 and 245 keV). Anterior and posterior whole-body scans were acquired with the patient supine at a speed of 5 cm/min using a matrix size of 256 × 1024. SPECT of the head and neck and of other districts eventually involved were performed using 6° steps, 40 s/step, a 180° orbit, and a matrix size of 64 × 64. Images were reconstructed iteratively using the ordered subsets-expectation maximization algorithm, and transaxial, coronal, and sagittal sections were obtained and analyzed.

Table 1 Number and anatomic site of metastatic lesions detected by CT and ¹⁸F-FDG-PET/CT in 25 patients with metastatic medullary thyroid carcinoma

Anatomic site	CT	¹⁸ F-FDG-PET/CT true positive ^a
Lymph nodes	79	59 (7)
Bone	14	7 (1)
Lung nodules	11	7
Micronodular lung involvement	7	0
Liver	10	5
Pancreas	4	1 (1)
Brain	2	0
Thyroid bed	4	4
Total	131	83 (9)

^a Lesions corresponding to CT abnormalities and in parenthesis those confirmed at subsequent follow-up

Results

Contrast-enhanced CT detected a total of 131 lesions in 25 patients with MMTC and Table 1 lists the anatomic sites of metastatic lesions. Among the 131 lesions detected by CT, 79 were enlarged lymph nodes and 14 were located in the bones. Lung metastases were detected by CT as 11 discrete lung nodules and in 7 cases as diffuse micronodular lung involvement. Furthermore, CT detected additional lesions in liver, pancreas, brain and thyroid bed as reported in Table 1.

A total of 92 lesions were detected by ¹⁸F-FDG-PET/CT of which 83 were also seen on CT and 9 were identified only by ¹⁸F-FDG-PET/CT (Table 1). Of the 83 lesions detected by both CT and ¹⁸F-FDG-PET/CT, 59 were located in lymph nodes enlarged on CT and 7 corresponded to bone abnormalities on CT. ¹⁸F-FDG-PET/CT failed to detect micronodular lung involvement and brain metastases. Compared to the CT findings, ¹⁸F-FDG-PET/CT detected 74.6 % of

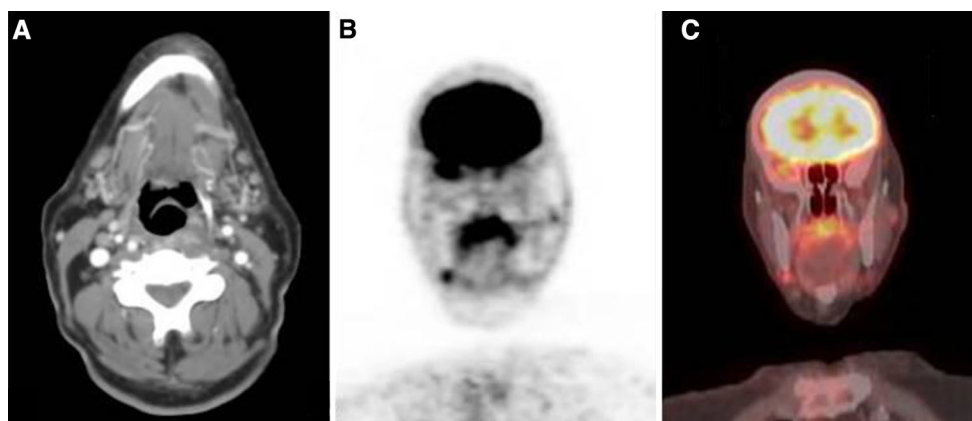


Fig. 1 Multimodal imaging performed in the same patient with MMTC: transaxial contrast-enhanced CT image (a); coronal PET (b) and fusion (c) images of the head by ¹⁸F-FDG-PET/CT scan. The

right submandibular lymph node showing focal ¹⁸F-FDG uptake on PET and fusion images is not enlarged on CT

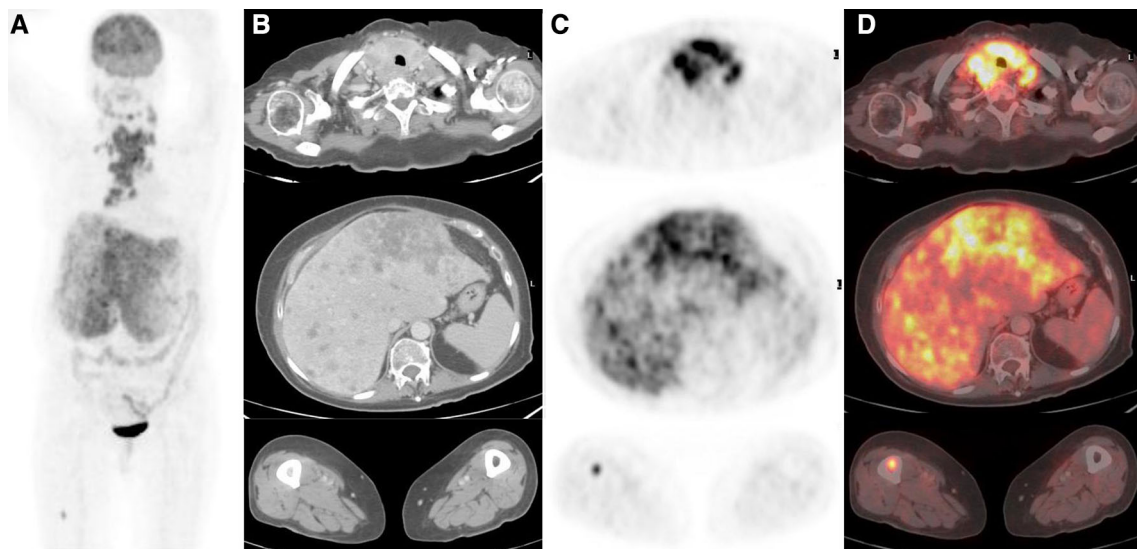
Table 2 SUV_{max} values of metastatic lesions detected by ¹⁸F-FDG-PET/CT in 25 patients with metastatic medullary thyroid carcinoma

Anatomic site	SUV _{max} Mean ± SD	SUV _{max} Range
Lymph nodes	3.6 ± 1.3	1.5–8.4
Bone	5.6 ± 1.2	3.4–7.0
Lung nodules	4.1 ± 2.6	1.1–7.5
Liver	5.3 ± 2.0	4.0–8.3
Pancreas	3.1 ± 0.5	2.7–3.5
Thyroid bed	5.0 ± 3.3	3.2–10.0
Total	4.0 ± 1.7	1.1–10.0

lymph node metastases, 50 % of bone lesions, 63.6 % of metastatic lung nodules, 50 % of liver lesions, 25 % of pancreatic lesions and 100 % of recurrences in the thyroid

Fig. 3 Multimodal imaging performed in the same patient with MMTC: transaxial contrast-enhanced CT images (a); coronal PET (b) and fusion (c) images of the thorax of ¹⁸F-FDG-PET/CT scan; SPECT images of the thorax performed 24 h after ¹¹¹In-Octreotide administration (d). The first and third columns show a left paratracheal lymph node and a right hilar lymph node, respectively, both enlarged on CT and showing focal ¹⁸F-FDG and ¹¹¹In-Octreotide uptake while the second column displays a prevascular lymph node not enlarged on CT showing focal ¹⁸F-FDG uptake but no ¹¹¹In-Octreotide uptake

bed. Seven of the 9 additional lesions detected by ¹⁸F-FDG-PET/CT were found in lymph nodes not enlarged on CT. All the additional lesions were confirmed by subsequent CT scan or conventional imaging performed at follow-up. Figure 1 shows representative images of CT and ¹⁸F-FDG-PET/CT in a patient with an ¹⁸F-FDG avid submandibular lymph node not enlarged on CT.

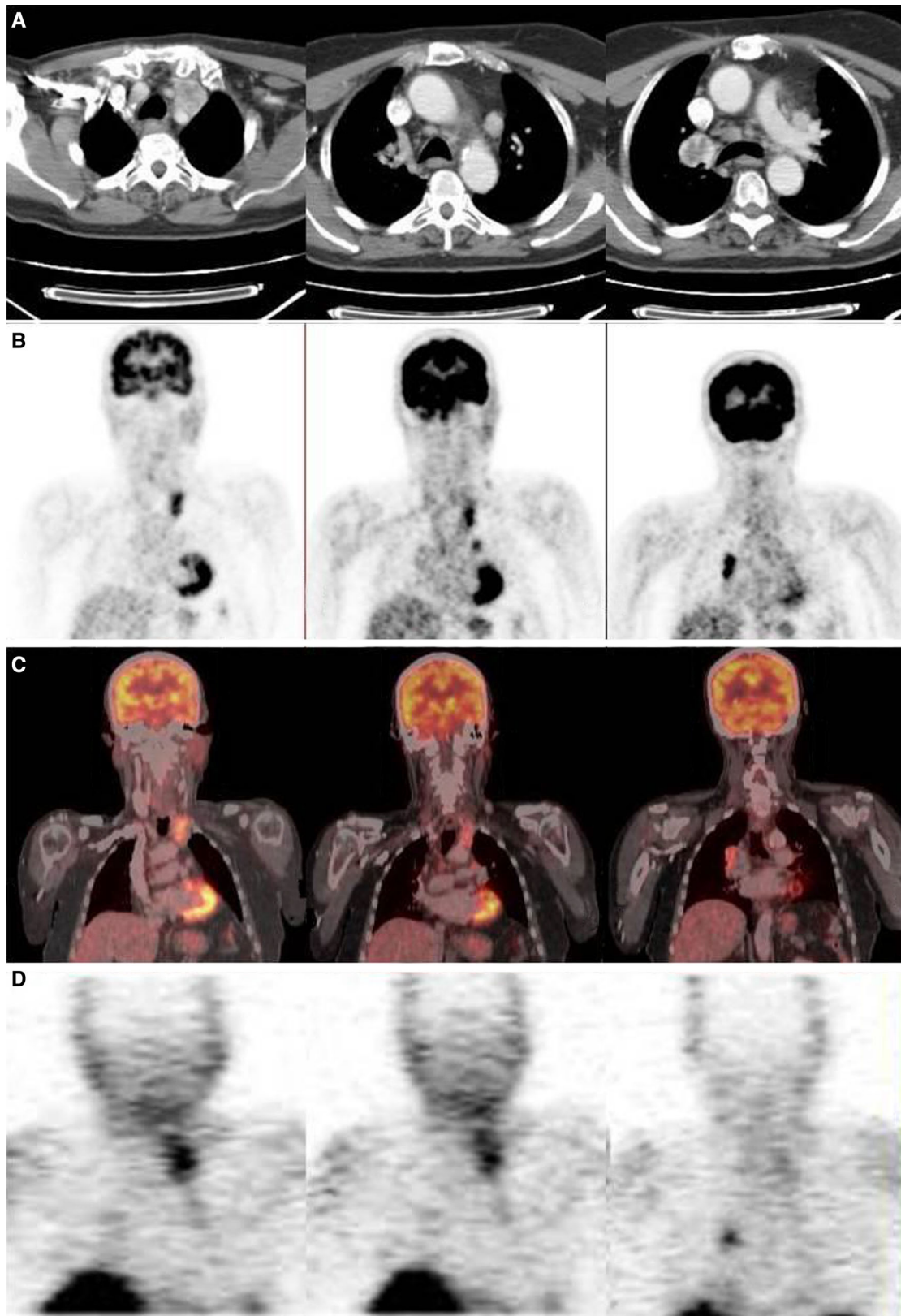
**Fig. 2** ¹⁸F-FDG-PET/CT scan performed in a patient with aggressive MMTC: maximum intensity projection view (a); transaxial contrast-enhanced CT (b), PET (c) and fusion (d) images showing metastatic

sites highly FDG-avid in the thoracic lymph nodes: SUV_{max} 8.4 (first row), in the liver: SUV_{max} 8.1 (second row) and in the right femur: SUV_{max} 5.2 (third row)

Table 3 Number and anatomic site of metastatic lesions detected by ¹⁸F-FDG-PET/CT and ¹¹¹In-Octreotide SPECT in 20 patients with metastatic medullary thyroid carcinoma

Anatomic site	¹⁸ F-FDG-PET/CT true positive ^a	¹¹¹ In-Octreotide SPECT true positive ^a
Lymph nodes	43	27
Bone	7	10
Lung nodules	7	6
Micronodular lung involvement	0	0
Liver	3	1
Pancreas	1	0
Brain	0	0
Thyroid bed	3	2
Total	64	46

^a Lesions corresponding to CT abnormalities or confirmed at subsequent follow-up



The mean value of SUV_{max} of all metastatic lesions was 4.0 ± 1.7 (SD). Table 2 reports the values of SUV_{max} and range in relation to the anatomic sites of lesions. In particular the SUV_{max} of lymph node metastases, which constituted the majority of metastatic lesions, was 3.6 ± 1.3 (mean \pm SD). The highest mean SUV_{max} values were found in bone lesions (5.6 ± 1.2 , mean \pm SD). In the whole series of patients, the range of SUV_{max} values varied between 1.1 and 10.0 and the highest values were obtained in patients with highly aggressive and advanced disease. Figure 2 shows representative images of ^{18}F -FDG-PET/CT in a patient with highly FDG-avid metastatic sites. Furthermore in 14 of 25 patients with calcitonin levels greater than 1000 pg/ml, SUV_{max} values of the most FDG-avid lesion in each patient were significantly higher than those of patients with calcitonin levels lower than 1000 pg/ml (5.72 ± 2.60 vs 3.07 ± 2.41 , $p = 0.02$).

^{111}In -Octreotide SPECT showed a total of 57 areas of tracer uptake in 20 metastatic MTC patients. ^{111}In -Octreotide uptake was detected in 24 of 52 lymph nodes enlarged on CT and in 6 additional lymph nodes. Furthermore, ^{111}In -Octreotide SPECT showed focal tracer uptake in 10 of 14 bone abnormalities found on CT. In the lungs, 6 of 11 nodules showed focal uptake of ^{111}In -Octreotide whereas diffuse tracer uptake not corresponding to CT abnormalities was found in one case. Only 1 liver lesion out of 7 hypodense liver lesions on CT was detected by ^{111}In -Octreotide SPECT whereas no tracer uptake was observed in 2 brain metastases or in 3 pancreatic lesions detected by CT. Focal uptake of ^{111}In -Octreotide was detected in 2 local recurrences of 3 confirmed on CT whereas diffuse tracer uptake was found in the thyroid bed of 7 additional cases in the absence of CT abnormalities. Among the 14 lesions detected by ^{111}In -Octreotide SPECT not corresponding to CT abnormalities only 3 lymph nodes were confirmed on CT or conventional imaging performed at follow-up. Table 3 reports the true positive results of

^{111}In -Octreotide SPECT and ^{18}F -FDG-PET/CT in the same subgroup of 20 patients. ^{18}F -FDG-PET/CT detected more lymph node metastases as compared to ^{111}In -Octreotide SPECT, whereas bone metastases were better detected by ^{111}In -Octreotide SPECT than by ^{18}F -FDG-PET/CT. Figure 3 shows representative images of CT, ^{18}F -FDG-PET/CT and ^{111}In -Octreotide SPECT performed in the same patient with multiple metastatic lymph nodes. Figure 4 shows multimodal imaging findings in an MTC patient with osteoblastic bone metastases.

Discussion

The present study shows that the addition of ^{18}F -FDG-PET/CT to conventional imaging may contribute to identifying lymph node involvement in metastatic MTC patients. Compared to contrast-enhanced CT, the overall sensitivity of ^{18}F -FDG-PET/CT was 63.4 %. When considering lymph node metastases, the sensitivity of ^{18}F -FDG-PET/CT increased to 74.6 % and additional lymph nodes not enlarged on CT could be identified as metastatic foci by ^{18}F -FDG-PET/CT. The majority of metastatic sites in our series of patients were found in lymph nodes and ^{18}F -FDG-PET/CT provided additional information in the evaluation of this prominent anatomic district. In agreement with previous studies [7, 31, 32], the contribution of ^{18}F -FDG-PET/CT in the evaluation of diffuse micronodular lung involvement, liver and brain metastases was limited due to the small size of the lesions or to low tumor-to-background ratios. In relation to bone metastases ^{18}F -FDG-PET/CT was able to detect osteolytic lesions but was limited by the osteoblastic nature of bone lesions from well-differentiated and slow-growing tumors as reported by previous studies [33].

The addition of ^{111}In -Octreotide SPECT to the evaluation of metastatic MTC patients did not provide relevant

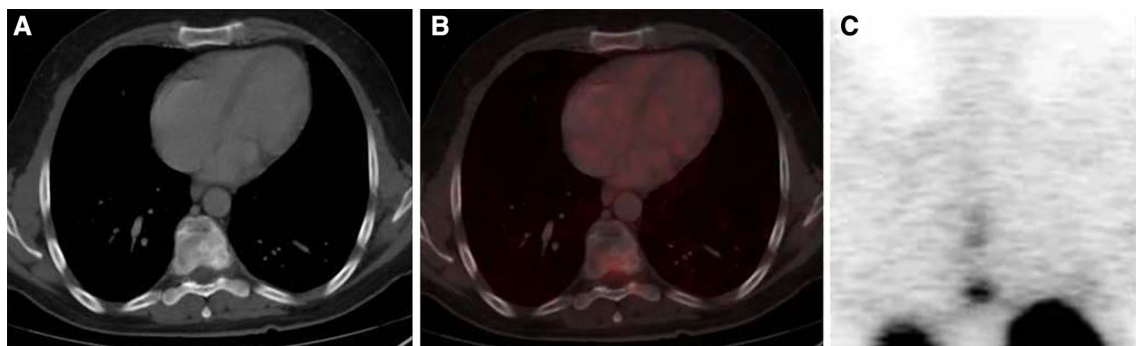


Fig. 4 Multimodal imaging performed in the same patient with MTC: transaxial contrast-enhanced CT (a) and fusion (b) images of ^{18}F -FDG-PET/CT scan; SPECT image of the thorax performed 24 h

after ^{111}In -Octreotide administration (c). The eighth dorsal vertebra shows CT abnormalities and intense focal ^{111}In -Octreotide uptake but no significant ^{18}F -FDG uptake

information on the extension of the disease but allowed characterization of the somatostatin receptor status of primary tumors and metastatic sites especially bone lesions. ^{111}In -Octreotide SPECT showed indeed a higher sensitivity in the detection of bone lesions than in revealing metastases of any other anatomic district indicating a high incidence or density of SST2 receptors in these lesions. Furthermore, ^{111}In -Octreotide SPECT detected more bone lesions than ^{18}F -FDG-PET/CT in the same patients providing additional functional information to evaluate metastatic dissemination to the bones. The main clinical application of ^{111}In -Octreotide SPECT is in the selection of candidates for treatment with both cold and radiolabeled somatostatin analogs as a high tracer uptake is a prerequisite for peptide receptor radionuclide therapy (PRRT) [34, 35]. In this setting, our study confirmed that ^{111}In -Octreotide SPECT can be employed to assess somatostatin receptor expression in tumor lesions and showed that it can be successfully used to identify bone lesions that are not definitely recognized as metastatic foci by other imaging techniques. Furthermore, it has been reported that somatostatin receptor scintigraphy is a better tool for monitoring the bone lesion response to PRRT than CT [36].

Imaging modalities are of primary importance in patients with metastatic MTC because, in agreement with current clinical guidelines, only those with significant tumor burden or symptomatic/progressive disease are candidates for systemic treatment. Patients with known metastases not candidates for systemic treatment are usually monitored by measurements of serum tumor markers and by repeated imaging procedures in order to assess disease progression. A large spectrum of imaging modalities may be employed to guide treatment decisions in individual patients. Depending on the anatomic sites of metastatic involvement ultrasound may be used for periodical evaluation of neck and liver; CT may be employed to monitor disease in the neck, chest and liver; bone metastases may be evaluated by bone scan and MRI of spine and pelvis. In addition, various functional imaging methodologies have been tested in MTC patients. In the last years, ^{68}Ga PET with somatostatin analogs such as DOTATOC, DOTATATE and DOTANOC have been proposed, in particular ^{68}Ga -DOTATATE PET/CT was shown to successfully localize recurrent or metastatic disease in a small series of MTC patients with calcitonin levels >1000 pg/ml [37], although, the routine use of these compounds is still limited. ^{18}F -fluorodeoxyphenylalanine (^{18}F -FDOPA) is currently considered the only nuclear medicine methodology capable of detecting recurrence in MTC patients with calcitonin values around 150 pg/mL [32], despite which its use is limited by its expense and uncertain supply. Other functional techniques such as $^{99\text{m}}\text{Tc}$ -dimer-captosuccinic acid ($^{99\text{m}}\text{Tc}$ -DMSA) scintigraphy or $^{131}\text{I}/^{123}\text{I}$ -metaiodobenzylguanidine ($^{131}\text{I}/^{123}\text{I}$ -MIBG) scintigraphy are

reported not to be recommended in MTC patients due to their low sensitivity in this neoplastic disease [26, 37].

Our study shows that ^{18}F -FDG-PET/CT may provide additional information on lymph node involvement and disease progression in this district. In agreement with previous studies, we found that ^{18}F -FDG uptake in metastatic lesions of MTC patients is usually low showing a mean SUV_{max} value of 4.0 ± 1.7 . This may limit the detectability of small lesions and the assessment of metabolic tumor response to treatment using ^{18}F -FDG-PET/CT. However, the large range of SUV_{max} values found in our study indicates that ^{18}F -FDG-PET/CT can identify patients with highly aggressive disease and guide individual-based therapeutic interventions.

In conclusion multimodal imaging with ^{18}F -FDG-PET/CT and ^{111}In -Octreotide SPECT may improve the management of MMTC patients by providing additional information on disease extension and progression in specific anatomic districts.

Acknowledgments This work was partly supported by Ministry of University and Research, MERIT—Medical Research in Italy (Project No. RBNE08YFN3_008); AIRC, Associazione Italiana per la Ricerca sul Cancro (Project No. 11756); POR (Programma Operativo Regionale) Campania FESR (Fondo Europeo Sviluppo Regionale) 2007/2013, Rete delle Biotecnologie Campane.

Compliance with ethical standards

Conflict of interest No potential conflicts of interest were disclosed.

References

- Schlumberger M, Carlomagno F, Baudin E, Bidart JM, Santoro M. New therapeutic approaches to treat medullary thyroid carcinoma. *Nat Clin Pract Endocrinol Metab.* 2008;4:22–32.
- Roy M, Chen H, Sippel RS. Current understanding and management of medullary thyroid cancer. *Oncologist.* 2013;18:1093–100.
- Elisei R, Pinchera A. Advances in the follow-up of differentiated or medullary thyroid cancer. *Nat Rev Endocrinol.* 2012;8:466–75.
- Giraudet AL, Al Ghulzan A, Auperin A, Leboulleux S, Chehboun A, Troalen F, et al. Progression of medullary thyroid carcinoma: assessment with calcitonin and carcinoembryonic antigen doubling times. *Eur J Endocrinol.* 2008;158:239–46.
- Schlumberger M, Bastholt L, Dralle H, Jarzab B, Pacini F, Smit JW, et al. 2012 European thyroid association guidelines for metastatic medullary thyroid cancer. *Eur Thyroid J.* 2012;1:5–14.
- Wells SA Jr, Asa SL, Dralle H, Elisei R, Evans DB, Gagel RF, et al. Revised American Thyroid Association guidelines for the management of medullary thyroid carcinoma. *Thyroid.* 2015;25:567–610.
- Giraudet AL, Vanel D, Leboulleux S, Auperin A, Dromain C, Chami L, et al. Imaging medullary thyroid carcinoma with persistent elevated calcitonin levels. *J Clin Endocrinol Metab.* 2007;92:4185–90.

8. Ganeshan D, Paulson E, Duran C, Cabanillas ME, Busaidy NL, Charnsangavej C. Current update on medullary thyroid carcinoma. *Am J Roentgenol*. 2013;201:W867–76.
9. Treglia G, Villani MF, Giordano A, Rufini V. Detection rate of recurrent medullary thyroid carcinoma using fluorine-18 fluorodeoxyglucose positron emission tomography: a meta-analysis. *Endocrine*. 2012;42:535–45.
10. Cheng X, Bao L, Xu Z, Li D, Wang J, Li Y. ¹⁸F-FDG-PET and ¹⁸F-FDG-PET/CT in the detection of recurrent or metastatic medullary thyroid carcinoma: a systematic review and meta-analysis. *J Med Imaging Radiat Oncol*. 2012;56:136–42.
11. Skoura E, Datsis IE, Rondogianni P, Tsagarakis S, Tzanela M, Skilakaki M, et al. Correlation between calcitonin levels and [(18)F]FDG-PET/CT in the detection of recurrence in patients with sporadic and hereditary medullary thyroid cancer. *ISRN Endocrinol*. 2012;2012:375231.
12. Gomez-Camarero P, Ortiz-de Tena A, Borrego-Dorado I, Vazquez-Albertino RJ, Navarro-Gonzalez E, Ruiz-Franco-Baux JV, et al. Evaluation of efficacy and clinical impact of ¹⁸F-FDG-PET in the diagnosis of recurrent medullary thyroid cancer with increased calcitonin and negative imaging test. *Rev Esp Med Nucl Imagen Mol*. 2012;31:261–6.
13. Ozkan E, Soydal C, Kucuk ON, Ibis E, Erbay G. Impact of (18)F-FDG PET/CT for detecting recurrence of medullary thyroid carcinoma. *Nucl Med Commun*. 2011;32:1162–8.
14. Palaniswamy SS, Subramanyam P. Diagnostic utility of PET/CT in thyroid malignancies: an update. *Ann Nucl Med*. 2013;27:681–93.
15. Wells SA Jr, Gosnell JE, Gagel RF, Moley J, Pfister D, Sosa JA, et al. Vandetanib for the treatment of patients with locally advanced or metastatic hereditary medullary thyroid cancer. *J Clin Oncol*. 2010;28:767–72.
16. Elisei R, Schlumberger MJ, Muller SP, Schoffski P, Brose MS, Shah MH, et al. Cabozantinib in progressive medullary thyroid cancer. *J Clin Oncol*. 2013;31:3639–46.
17. Lam ET, Ringel MD, Kloos RT, Prior TW, Knopp MV, Liang J, et al. Phase II clinical trial of sorafenib in metastatic medullary thyroid cancer. *J Clin Oncol*. 2010;28:2323–30.
18. Maxwell JE, Sherman SK, O'Dorisio TM, Howe JR. Medical management of metastatic medullary thyroid cancer. *Cancer*. 2014;120:3287–301.
19. Contractor KB, Aboagye EO. Monitoring predominantly cytostatic treatment response with ¹⁸F-FDG PET. *J Nucl Med*. 2009;50(Suppl 1):97S–105S.
20. Walter MA, Benz MR, Hildebrandt IJ, Laing RE, Hartung V, Damoiseaux RD, et al. Metabolic imaging allows early prediction of response to vandetanib. *J Nucl Med*. 2011;52:231–40.
21. Reubi JC, Schonbrunn A. Illuminating somatostatin analog action at neuroendocrine tumor receptors. *Trends Pharmacol Sci*. 2013;34:676–88.
22. Mato E, Matias-Guiu X, Chico A, Webb SM, Cabezas R, Berna L, et al. Somatostatin and somatostatin receptor subtype gene expression in medullary thyroid carcinoma. *J Clin Endocrinol Metab*. 1998;83:2417–20.
23. Papotti M, Kumar U, Volante M, Pecchioni C, Patel YC. Immunohistochemical detection of somatostatin receptor types 1–5 in medullary carcinoma of the thyroid. *Clin Endocrinol (Oxf)*. 2001;54:641–9.
24. Christian JA, Cook GJ, Harmer C. Indium-111-labelled octreotide scintigraphy in the diagnosis and management of non-iodine avid metastatic carcinoma of the thyroid. *Br J Cancer*. 2003;89:258–61.
25. Baudin E, Lumbroso J, Schlumberger M, Leclere J, Giammarile F, Gardet P, et al. Comparison of octreotide scintigraphy and conventional imaging in medullary thyroid carcinoma. *J Nucl Med*. 1996;37:912–6.
26. Gao Z, Biersack HJ, Ezziddin S, Logvinski T, An R. The role of combined imaging in metastatic medullary thyroid carcinoma: ¹¹¹In-DTPA-octreotide and ¹³¹I/123I-MIBG as predictors for radionuclide therapy. *J Cancer Res Clin Oncol*. 2004;130:649–56.
27. Lodish M, Dagalakis U, Chen CC, Sinaii N, Whitcomb P, Aikin A, et al. (111)In-octreotide scintigraphy for identification of metastatic medullary thyroid carcinoma in children and adolescents. *J Clin Endocrinol Metab*. 2012;97:E207–12.
28. Rufini V, Calcagni ML, Baum RP. Imaging of neuroendocrine tumors. *Semin Nucl Med*. 2006;36:228–47.
29. De Luca S, Fonti R, Palmieri G, Federico P, Del Prete G, Pacelli R, et al. Combined imaging with ¹⁸F-FDG-PET/CT and ¹¹¹In-labeled octreotide SPECT for evaluation of thymic epithelial tumors. *Clin Nucl Med*. 2013;38:354–8.
30. Fonti R, Larobina M, Del Vecchio S, De Luca S, Fabbri R, Catalano L, et al. Metabolic tumor volume assessed by ¹⁸F-FDG PET/CT for the prediction of outcome in patients with multiple myeloma. *J Nucl Med*. 2012;53:1829–35.
31. Treglia G, Castaldi P, Villani MF, Perotti G, de Waure C, Filice A, et al. Comparison of ¹⁸F-DOPA, ¹⁸F-FDG and ⁶⁸Ga-somatostatin analogue PET/CT in patients with recurrent medullary thyroid carcinoma. *Eur J Nucl Med Mol Imaging*. 2012;39:569–80.
32. Slavikova K, Montravers F, Treglia G, Kunikowska J, Kaliska L, Vereb M, et al. What is currently the best radiopharmaceutical for the hybrid PET/CT detection of recurrent medullary thyroid carcinoma? *Curr Radiopharm*. 2013;6:96–105.
33. Chua S, Gnanasegaran G, Cook GJ. Miscellaneous cancers (lung, thyroid, renal cancer, myeloma, and neuroendocrine tumors): role of SPECT and PET in imaging bone metastases. *Semin Nucl Med*. 2009;39:416–30.
34. Brabander T, Kwekkeboom DJ, Feelders RA, Brouwers AH, Teunissen JJ. Nuclear medicine imaging of neuroendocrine tumors. *Front Horm Res*. 2015;44:73–87.
35. van Essen M, Sundin A, Krenning EP, Kwekkeboom DJ. Neuroendocrine tumours: the role of imaging for diagnosis and therapy. *Nat Rev Endocrinol*. 2014;10:102–14.
36. van Vliet EI, Hermans JJ, de Ridder MA, Teunissen JJ, Kam BL, de Krijger RR, et al. Tumor response assessment to treatment with [¹⁷⁷Lu-DOTA0, Tyr3]octreotate in patients with gastroenteropancreatic and bronchial neuroendocrine tumors: differential response of bone versus soft-tissue lesions. *J Nucl Med*. 2012;53:1359–66.
37. Ozkan ZG, Kuyumcu S, Uzum AK, Gecer MF, Ozel S, Aral F, et al. Comparison of (68)Ga-DOTATATE PET–CT, (18)F-FDG PET–CT and ^{99m}Tc-(V)DMSA scintigraphy in the detection of recurrent or metastatic medullary thyroid carcinoma. *Nucl Med Commun*. 2015;36:242–50.